Original Article

Silencing of the long non-coding RNA MEG3 suppresses the apoptosis of aortic endothelial cells in mice with chronic intermittent hypoxia via downregulation of HIF-1α by competitively binding to microRNA-135a

Haibo Ding, Jiefeng Huang, Dawen Wu, Jianming Zhao, Jianchai Huang, Qichang Lin

Department of Respiratory and Critical Care Medicine, The First Affiliated Hospital of Fujian Medical University, Fuzhou 350004, China

Contributions: (I) Conception and design: H Ding, J Huang, D Wu; (II) Administrative support: H Ding, D Wu, J Zhao; (III) Provision of study materials or patients: H Ding, J Huang; (IV) Collection and assembly of data: J Huang, D Wu, Q Lin; (V) Data analysis and interpretation: J Zhao, J Huang, Q Lin; (VI) Manuscript writing: All authors; (VII) Final approval of manuscript: All authors.

Correspondence to: Haibo Ding. Department of Respiratory and Critical Care Medicine, The First Affiliated Hospital of Fujian Medical University, No. 20, Chazhong Road, Fuzhou 350004, China. Email: dinghaibo73@126.com.

Background: Chronic intermittent hypoxia (CIH) involves substantial cortico-hippocampal injury, causing impairments of neurocognitive, respiratory, and cardiovascular functions. Long non-coding RNAs (lncRNAs) participate in CIH functions and development. Therefore, we explored the mechanisms involving lncRNA maternally expressed gene 3 (MEG3) regulating the aortic endothelial function of CIH mice via regulation of microRNA-135a (miR-135a) and the hypoxia-inducible factor (HIF)-1α.

Methods: Expression of MEG3, miR-135a, and HIF-1α in CIH mice and CIH-treated cells was detected. Then, the apoptosis and proliferation of the aortic endothelial cells were examined to verify whether miR-135a and HIF-1α participated in CIH. Next, the interactions between MEG3, miR-135a, and HIF-1α were explored. Later, the effects of MEG3/miR-135a/HIF-1α on the expression of proliferation- and apoptosis-related factors and aortic injury were investigated *via* gain- and loss-of function studies both *in vivo* and *in vitro*.

Results: MEG3 and HIF-1α were highly expressed while miR-135a was poorly expressed in CIH mice and CIH-modeled cells. Moreover, miR-135a targeted HIF-1α to promote cell proliferation and inhibit apoptosis. MEG3 regulated HIF-1α expression by competitively binding to miR-135a. More importantly, we found that the silencing of MEG3/HIF-1α and the overexpression of miR-135a inhibited the apoptosis and injury of aortic endothelial cells while promoting cell proliferation in CIH mice.

Conclusions: Altogether, silencing of MEG3 suppressed the aortic endothelial injury and cell apoptosis in CIH mice by downregulating HIF-1α through sponging miR-135a, providing evidence of a potential therapeutic target for CIH.

Keywords: Maternally expressed gene 3 (MEG3); microRNA-135a (miR-135a); hypoxia-inducible factor 1α; chronic intermittent hypoxia (CIH); aortic endothelial cells; apoptosis

Submitted Jul 30, 2019. Accepted for publication Jan 01, 2020.
doi: 10.21037/jtd-19-2472
View this article at: http://dx.doi.org/10.21037/jtd-19-2472

Introduction

Chronic intermittent hypoxia (CIH) or intermittent hypoxia (IH) has been a popular research subject for decades and represents a pathological symptom that leads to the disorder of detrimental and beneficial effects on many physiological systems characterized by recurrent episodes of hypoxia interspersed with periods of normoxia (1). It has been

previously reported that CIH could lead to vascular injuries, such as arterial endothelial cell apoptosis (2). Moreover, CIH has been shown to result in aortic injury with features of oxidative stress and inflammatory reaction (3). Also, CIH has been found to be involved in the regulation of gene expression in human aortic endothelial cells (4). In terms of the approaches to treat the CIH-induced endothelial cell apoptosis, it has been reported that taurodeoxycholic acid (TUDCA) could alleviate endothelial cell apoptosis (5). However, effective and specific treatments for aortic endothelial dysfunction in CIH have not been found yet, indicating that more studies are required to discover the mechanisms for treating aortic endothelial dysfunction induced by CIH.

Hypoxia-inducible factor (HIF)-1α has been found to be involved in transcriptional level regulation in CIH (6). Moreover, the targeting relationship between HIF-1α and microRNA-135a (miR-135a) has also been revealed by previous evidence (7). It has been observed that CIH results in differential expression of microRNAs (miRNAs) that regulate genes related to apoptosis or autophagy (8). More importantly, miR-135a-3p mediates angiogenesis and tissue repair through modulation of the p38 pathway in endothelial cells (9). Additionally, some long non-coding RNAs (lncRNAs) have been found to participate in regulatory processes of endothelial progression and function, such as the lncRNA SENCR involved in human vascular endothelial cell (HUVEC) development (10). A previous study demonstrated that maternally expressed gene 3 (MEG3) was expressed in pulmonary artery smooth muscle cells (PASMCs) and participated in cell progression under hypoxia (11). Furthermore, the correlation between MEG3 and some miRNAs in diverse diseases demonstrated that MEG3 regulates cell migration and apoptosis by sponging miR-548d-3p in oral squamous cell carcinoma (12). Moreover, MEG3 inhibited the proliferation and migration of endothelial cells by mediating miR-21 (13). Based on the findings mentioned above, we elaborated the hypothesis that MEG3 affects aortic endothelial function and cell apoptosis in CIH mice by regulating HIF-1α though interacting with miR-135a, and we aimed to confirm this hypothesis to provide clinical insight for the treatment of aortic endothelial dysfunction in CIH.

Methods

Ethics statement

All animal experiments were performed following the principles and procedures of the Guide for the Care and Use of Laboratory Animals by the National Institutes of Health. This study was approved by the Animal Ethics Committee of The First Affiliated Hospital of Fujian Medical University (No. 201806003).

Establishment of the CIH mouse model and animal treatment

A total of 60 C57BL/6 mice aged 6–7 weeks with a weight of 20–25 g (Shanghai Laboratory Animal Center, Chinese Academy of Sciences, Shanghai, China) were used for this study. The CIH mouse model was established as described by previous studies (14,15). Initially, 54 modeled mice were selected during IH and the FiO_2 was decreased from 2% to 6.5% within a 30 s period followed by a rapid return to 21% within a subsequent 30 s period. This regimen of IH induced oxyhemoglobin desaturation from 99% to 70% (60 times/h) (15,16). The remaining 6 mice used as control were similarly exposed to air. The mice underwent CIH treatment in illumination period (9 a.m. to 9 p.m.) to match the sleep cycle of mice. Next, LV5-GFP (lentivirus vector overexpressing gene) or pSIH1-H1-copGFP [lentivirus short hairpin RNA (shRNA) fluorescence expression vector silencing gene] was used to construct the gene lentivirus vector and miR-135a was overexpressed using agomir. The lentivirus vectors and agomir were provided by Shanghai GenePharma Co., Ltd. (Shanghai, China). After that, the CIH mice were injected with agomir-negative control (NC), miR-135a agomir, sh-NC, sh-HIF-1α or sh-MEG3. This experiment lasted 30 days, and the mice were weighed and recorded before being fed at 9 a.m. on the 1st, 7th, 14th, 21st and 28th day of the experiment. The mice were euthanized to collect the aorta tissues for hematoxylin-eosin (HE) staining and immunohistochemistry. Meanwhile, 0.5 mL of blood was extracted from aorta of mice and then used for blood gas analysis using an i-STAT blood gas analyzer (i-stat300, Abbott Laboratories, Chicago, Illinois, USA).

HE staining

The aorta arch tissues were sectioned, dewaxed by xylene and dehydrated. Then, the sections were immersed in hematoxylin for 5 min, in 1% hydrochloric ethanol for 30 s, and in 0.5% eosin for 3 min. Next, the sections were routinely treated and observed under the microscope.

Table 1 Primer sequences for RT-qPCR

Gene	Primer sequence (5'-3')
MEG3	F: CTGCCCATCTACACCTCACG
	R: CTCTCCGCCGTCTGCGCTAGGGGCT
HIF-1α	F: CTCGGCGAAGCAAAGAGT
	R: GCCATCTAGGGCTTTCAG
GAPDH	F: AATTCAACGGCACAGTCAAGG R: TGTTAGTGGGGTCTCGCTCC

RT-qPCR, reverse transcription quantitative polymerase chain reaction; MEG3, maternally expressed gene 3; HIF-1α, hypoxia-inducible factor 1α; GAPDH, glyceraldehyde 3-phosphate dehydrogenase.

Cell treatment

The aortic endothelial tissues of C57BL/6 male mice were sheared and washed with 0.01 mol/L of PBS (containing 1% penicillin-streptomycin), digested with 2.5 g/L of trypsin and 2 g/L of type II collagenase, and then inoculated into 6-well plates in a concentration of 1×10^8/L in 5% CO_2 at 37 ℃. Upon reaching 80% confluence, the cells (1×10^8 cells/L) were sub-cultured at a ratio of 1:3 and passaged. According to a previous study (5), the cells underwent CIH treatment. In brief, the cells were added with degermed absolute ethyl alcohol for preincubation for 30 min and then incubated in a Bio Spherix IH incubator (Ox 110) for 4 h with an oxygen concentration controlled in circulation of 21% for 55 s/5% for 55 s. Subsequently, the cells were subjected to CIH treatment or delivered with sh-MEG3, miR-135a mimic, oe-HIF-1α, miR-135a inhibitor or their respective NC individually or together. The mimic and controls were provided by Shanghai GenePharma Co., Ltd. (Shanghai, China).

RNA fluorescence in situ hybridization (FISH)

According to the instructions of the FISH kit (Roche, Basel, Swiss), the location of MEG3 subcellular was detected. Initially, the mouse endothelial cells were fixed with 4% polyformaldehyde and then cultured in medium containing digoxin labeled MEG3 probes (Sigma Aldrich, St. Louis, Mo, USA). Next, the cells were stained with 4', 6-diamino-2-phenylindole (Sigma Aldrich, St. Louis, Mo, USA) at room temperature for 10 min and photographed under a laser confocal microscope (FV1000, Olympus, Tokyo, Japan) to obtain the fluorescence images.

Dual-luciferase reporter gene assay

The 3'-untranslated region (UTR) fragments of HIF-1α were synthesized and introduced into a pGL3-reporter (Promega Corporation, Madison, WI, USA). The mutant (Mut) sites of the complementary sequence of the HIF-1α wild type (Wt) plasmid were designed and inserted into the pGL3-reporter plasmids. The pGL3-HIF-1α-Wt and pGL3-HIF-1α-Mut plasmids were respectively co-transfected with miR-135a mimic, miR-135a Mut, or miR-NC (all from Shanghai GenePharma Co., Ltd., Shanghai, China) into HEK293 cells (American Type Culture Collection, Manassas, VA, USA). The luciferase activity was then detected using a Luciferase kit (Promega Corporation, Madison, WI, USA). The relationship between MEG3 and miR-135a was examined using the same method.

RNA isolation and quantitation

Total RNA was extracted and transcribed into complementary DNA using a PrimeScript™ RT reagent kit with gDNA Eraser kit (RRO37A, Takara, Kyoto, Japan). Next, the expression of miR-135a and genes was examined following the instructions of the TaqMan miRNA Assay kit [4440886 (462760_mat) and 4427975 (002232), Thermo Fisher Scientific, Massachusetts, USA] and the SYBR®Premix Ex Taq™ kit (Tli RNaseH Plus) (RR820A Takara, Kyoto, Japan). The RT-qPCR was conducted using an ABI 7500 PCR instrument (Thermo Fisher Scientific).

With glyceraldehyde 3-phosphate dehydrogenase (GAPDH) used as the internal control for genes and U6 for miR-135a, the fold changes were calculated using the $2^{-\Delta\Delta Ct}$ method (17). The primers (*Table 1*) used in the experiment were provided by Shanghai GenePharma Co., Ltd. (Shanghai, China).

Western blot analysis

The aorta arch cells or endothelial cells of mice were mixed with the lysis buffer containing phenylmethylsulfonyl fluoride (PMSF) to isolate total protein. The proteins were then dissolved in 2× sodium dodecyl sulfate (SDS) loading buffer, separated by 10% SDS-polyacrylamide gel electrophoresis (SDS-PAGE) and transferred onto a polyvinylidene fluoride membrane. The membrane was incubated with primary antibodies rabbit anti-proliferating cell nuclear antigen (PCNA) (ab92552, 1:1,000), cleaved-caspase 3 (ab2302, 1:1,000), Bcl-2-associated X protein (Bax)

(ab182733, 1:2,000), B-cell lymphoma 2 (Bcl-2) (ab692, 1:500), HIF-1α (ab2185, 1:1,000), and β-actin (ab8226, 1:1,000) (all from Abcam, Cambridge, UK). Next, the membrane was washed with tris-buffered saline Tween-20 (TBST) and incubated with the horseradish peroxidase-labeled secondary rabbit anti-antibodies (HS201-01, Mouse; HS101-01; TransGen Biotech, Beijing, China) for 1 h. Then, the membrane was rinsed with TBST, developed using an enhanced chemiluminescence fluorescence detection kit (BB-3501, Amersham Pharmacia Biotech, Inc., Cambridge, UK) and photographed using a Bio-Rad Image Analysis System (Bio-Rad Laboratories, Hercules, CA, USA). The relative protein expression was calculated using the Quantity One v4.6.2 software.

RNA pull-down assay

The endothelial cells were transduced with biotinylated miR-135a-wt (bio-miR-135a-wt) (40 nmol/L), biotinylated miR-135a-mut (bio-miR-135a-mut), or biotinylated miR-NC (bio-miR-NC). After 48 h, the cells were incubated with the lysis buffer for 10 min. Next, the lysed cells were incubated at 4 ℃ for 4 h with streptavidin magnetic beads (Life Sciences Solutions Group, Thermo Fisher Scientific). Lastly, RNA was extracted using the Trizol method and the MEG3 expression was detected by RT-qPCR (18).

RNA immunoprecipitation (RIP) assay

The endothelial cells were lysed and centrifuged. Part of the cell extract was taken out as Input and the other part was co-precipitated with the rabbit anti-Ago2 (ab32381, 1:50, Abcam Inc., Cambridge, MA, USA). The magnetic bead-antibody compound was resuspended in 900 μL of RIP wash buffer and added with 100 μL of cell extract at 4 ℃ overnight. Lastly, both the samples and Input were treated with protease K to extract RNA.

TUNEL assay

Under a light microscope, the apoptotic cells were counted on at least 3 cell slides from each mouse. Using a DeadEnd™ fluorescence labeling TUNEL detection kit (Promega Corporation, Madison, WI, USA), the tissue sections were dewaxed, treated by freshly-prepared 2% H_2O_2 for 10 min, and added with 20 μg/mL of DNase-free protease K at 37 ℃ for 30 min. Next, the cells were added with 100 μL of balanced buffer for 10 min and incubated with 100 μL of terminal deoxynucleotidyl transferase (TdT) at 37 ℃ for 60 min in dark. After that, the sections were incubated with the labeled stop solution for 10 min and pre-stained using 10 mg/mL of diamidino-phenyl-indole solution for 5 min. Under a laser scanning confocal microscope (Nikon Inc., Tokyo, Japan), the cell nucleus was stained blue and the positive apoptotic cells were stained green. A total of 5 high power fields were randomly selected in each section for counting apoptotic cells using the ImageProPlus medical image analysis system (Motic Med 6.0 system, USA).

EdU assay

The cells (4×10^4 cells/well) were incubated with EdU medium for 2 h, with fixation fluid for 30 min (100 μL/well), added with 2 mg/mL of glycine for 5-min incubation, and incubated with penetrating agent (PBS containing 0.5% TritonX-100) for 10 min. Then, the cells were incubated with 1× Apollo staining reaction solution for 30 min and with 1× Hoechst 33342 reaction fluid for 30 min, added with anti-fade mounting medium, and observed under a fluorescence microscope. The number of EdU-labeled cells was counted and the cells with red-stained nucleus were regarded as positive cells. Lastly, the number of positive and negative cells on 3 random visual fields was counted under the microscope.

Statistical analysis

All data were processed using the SPSS 21.0 statistical software. Measurement data were expressed as mean ± standard deviation. Data with normal distribution and homogeneity of variance were compared by unpaired *t*-test between two groups, by one-way analysis of variance (ANOVA) among multiple groups with Tukey's *post hoc* test. The data at different time points were compared using repeated measures ANOVA, followed by Bonferroni *post hoc* test. A $P<0.05$ was considered statistically significant.

Results

Successful establishment of the CIH mouse model

Initially, the mice underwent CIH treatment to explore changes of aorta of CIH mice. It was found that the body weight decreased in 14–28 d (*Figure 1A*) and levels of PaO_2 and SaO_2 of CIH-treated mice were significantly decreased

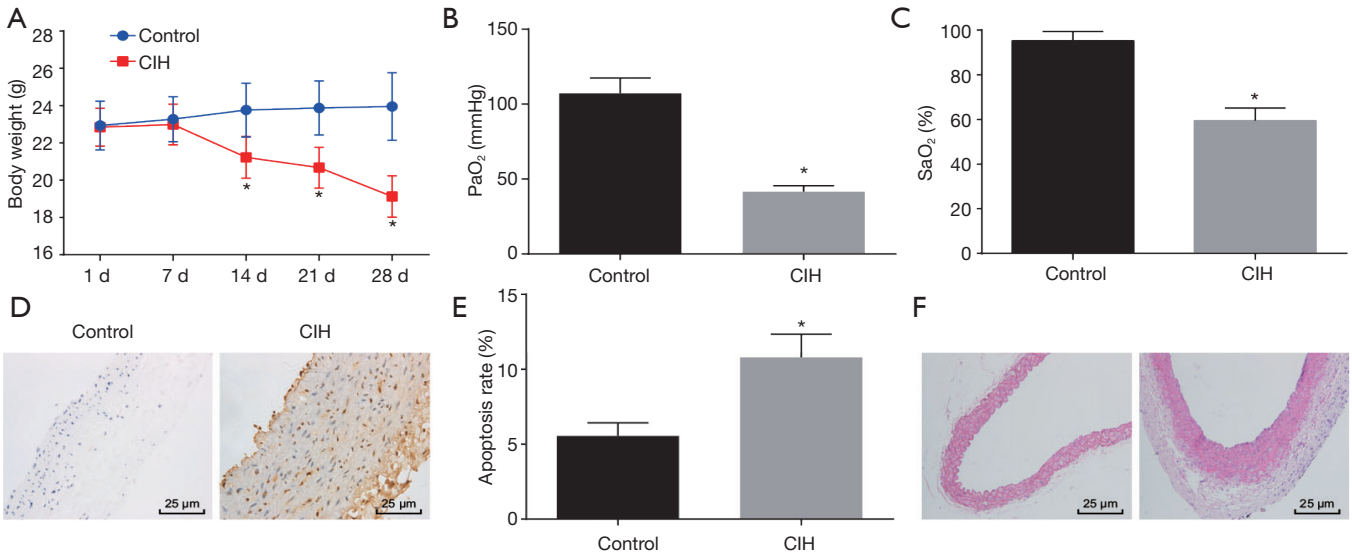

Figure 1 The CIH mouse model is successfully established. (A) The body weight of normal mice and CIH-treated mice. (B) The PaO_2 levels of normal mice and CIH-treated mice. (C) The SaO_2 levels of normal mice and CIH-treated mice. (D,E) Cell apoptosis of aorta arch of normal mice and CIH mice examined by TUNEL staining (400×). (F) The pathological changes of aorta arch of normal mice and CIH mice examined by HE staining (100×). *, P<0.05 compared with normal mice. The results were measurement data and expressed as mean ± standard deviation. The data in (A) were analyzed by repeated measures ANOVA and *post hoc* test was conducted using Bonferroni, and the data in (B,C,D,E) were analyzed using an unpaired *t*-test. N=6. CIH, chronic intermittent hypoxia; TUNEL, terminal deoxynucleotidyl transferase-mediated dUTP nick end-labeling; HE, hematoxylin-eosin; ANOVA, analysis of variance.

(*Figure 1B,C*) when compared to those of normal mice, suggesting that the CIH mouse model was successfully established. Moreover, TUNEL staining and HE staining were performed to examine the changes of aorta arch of normal mice and CIH mice. Compared with normal mice, the CIH mice exhibited higher positive rate of cells in the aorta arch (*Figure 1D,E*). The normal mice showed normal aorta tissue morphology and completely-arranged cells. In contrast, the CIH mice showed early pathological changes of atherosclerosis in aorta, partial deletion of endothelial cells, subendocardial foam cell deposition, obvious medial smooth muscle cell hyperplasia, disorder of cell arrangement, and thickening of the vessel wall (*Figure 1F*).

Upregulation of miR-135a enhances proliferation and represses apoptosis of CIH cells by targeting HIF-1α

An online website was used to analyze the miRNAs targeting HIF-1α to explore the upstream regulatory mechanism of HIF-1α. The results revealed miR-135a as a potential miRNA that regulated HIF-1α (*Figure 2A*). Moreover, the results from the RT-qPCR revealed that the CIH mice exhibited higher HIF-1α expression but lower miR-135a expression than normal mice (*Figure 2B*). Furthermore, the dual-luciferase reporter gene assay showed that miR-135a mimic decreased the luciferase activity of HIF-1α-Wt, while had no obvious effects on HIF-1α-Mut (*Figure 2C*).

To examine whether miR-135a and HIF-1α are involved in CIH, the endothelial cells of mice underwent CIH treatment and transfection. Through western blot analysis, increased HIF-1α expression was observed in endothelial cells after CIH treatment. Meanwhile, the HIF-1α expression in endothelial cells was inhibited by overexpression of miR-135a, but upregulated by the inhibition of miR-135a (*Figure 2D,E*). Therefore, the function of miR-135a/HIF-1α in cells after CIH treatment was explored through western blot analysis, EdU assay and TUNEL staining. The results obtained indicated that the CIH-treated cells exhibited lower PCNA and Bcl-2 expression and decreased cell proliferation, but higher cleaved-caspase 3 and Bax expression and increased cell apoptosis than cells without treatment. The same trend was found in CIH-treated cells delivered with both miR-135a

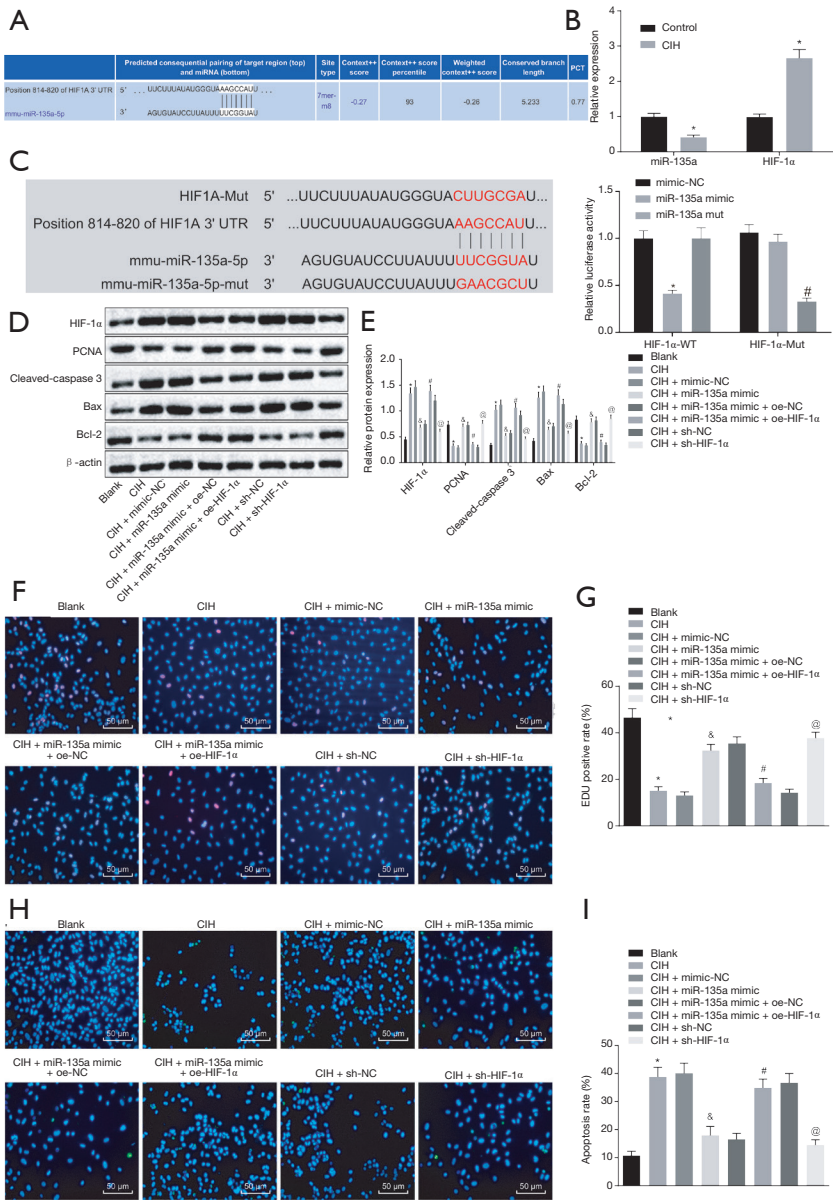

Figure 2 Overexpressed miR-135a improves proliferation and suppresses apoptosis of CIH cells by targeting HIF-1α. (A) The target relationship between miR-135a and HIF-1α analyzed using an online website. (B) Increased HIF-1α expression but decreased miR-135a expression in CIH mice examined by RT-qPCR (N=6). *, P<0.05 compared with normal mice. (C) miR-135a was verified to target HIF-1α by dual-luciferase reporter gene assay. *, P<0.05 compared with mimic-NC, #, P<0.05 compared with miR-135a mimic. (D,E) The effect of miR-135a on protein expression of HIF-1α, PCNA, Bcl-2, cleaved-caspase 3 and Bax examined by western blot analysis. (F,G) cell proliferation in cells with different treatments examined by EdU assay (×200). (H,I) Cell apoptosis after different treatments examined by TUNEL assay (×400). *, P<0.05 compared with cells without treatment; &, P<0.05 compared with CIH-treated cells delivered with mimic-NC; #, P<0.05 compared with CIH-treated cells delivered with both miR-135a mimic and oe-NC; @, P<0.05 compared with CIH-treated cells delivered with sh-NC. The results were measurement data and expressed as mean ± standard deviation. The data between two groups were analyzed using an unpaired *t*-test, while the comparisons among multiple groups were performed using ANOVA with *post hoc* test conducted by Tukey's. Experiment was repeated 3 times. CIH, chronic intermittent hypoxia; HIF-1α, hypoxia-inducible factor 1α; RT-qPCR, reverse transcription quantitative polymerase chain reaction; PCNA, proliferating cell nuclear antigen; Bcl-2, B-cell lymphoma 2; Bax, Bcl-2-associated X protein; EdU, 5-ethynyl-2'-deoxyuridine; TUNEL, terminal deoxynucleotidyl transferase-mediated dUTP nick end-labeling.

mimic and oe-HIF-1α than CIH-treated cells delivered with both miR-135a mimic and oe-NC (*Figure 2D,E,F,G,H,I*). Additionally, higher PCNA and Bcl-2 expression and increased cell proliferation, but lower cleaved-caspase 3 and Bax expression and decreased cell apoptosis were found in CIH-treated cells delivered with miR-135a mimic and sh-HIF-1α in contrast to the CIH-treated cells with mimic-NC and sh-NC, respectively (*Figure 2D,E,F,G,H,I*).

Silenced MEG3 downregulates HIF-1α by competitively binding to miR-135a during CIH

To explore whether lncRNA was involved in regulating HIF-1α by interacting with miR-135a, an online website was used to identify potential lncRNAs that interact with miR-135a, and it was found that MEG3 had the potential to interact with miR-135a (*Figure 3A*). The subcellular localization of MEG3 in endothelial cells by RNA-FISH, and the results show that MEG3 was mainly located in the cytoplasm (*Figure 3B*).

Subsequently, to demonstrate whether MEG3 could mediate the expression of HIF-1α by competitively binding to miR-135a, dual-luciferase reporter gene assay, RIP assay and RNA pull-down assay were conducted. The dual-luciferase reporter gene assay revealed that miR-135a mimic inhibited the luciferase activity of cells treated with MEG3-Wt but had no significant effect on cells treated with MEG3-Mut and miR-135a-Mut had no effect on the luciferase activity of MEG3-Wt but significantly reduced the luciferase activity of MEG3-Mut (*Figure 3C*).

The RNA pull-down assay showed that in Bio-miR-135a-Wt treated cells, the binding level of MEG3 and miR-135a was higher than that in cells treated with Bio-miR-NC or Bio-miR-135a-Mut (*Figure 3D*). After MEG3 was silenced, the binding level of HIF-1α to miR-135a was enhanced in the cells when compared with that of the cells treated with sh-NC (*Figure 3E*). The results suggested that MEG3 could bind to miR-135a to inhibit the binding of miR-135a to HIF-1α. The RIP assay further confirmed that MEG3 and miR-135a bound to the Ago2 protein, respectively (*Figure 3F*).

Besides, it revealed that MEG3 expression was upregulated in aorta tissues and endothelial cells of mice after CIH treatment (*Figure 3G*). Meanwhile, MEG3 silencing enhanced the inhibitory effects of miR-135a on HIF-1α expression (*Figure 3H*). Therefore, MEG3 regulated HIF-1α expression by competitively binding to miR-135a in CIH.

Downregulation of MEG3 improves the proliferation but represses the apoptosis of endothelial cells from CIH mice by upregulating miR-135a

In contrast to the CIH-treated cells delivered with sh-NC, the CIH-treated cells delivered with sh-MEG3 exhibited a higher expression of PCNA and Bcl-2 and increased proliferation, but lower expression of cleaved-caspase 3 and Bax along with decreased apoptosis. The same trend was observed in the CIH-treated cells delivered with both miR-135a inhibitor and sh-MEG3 compared to the CIH-treated cells delivered with both miR-135a inhibitor and sh-NC (*Figure 4A,B*). Furthermore, EdU staining (*Figure 4C,D*) and TUNEL staining (*Figure 4E,F*) revealed that in CIH-treated cells delivered with sh-MEG3, the cell proliferation (EdU positive cells) was increased and cell apoptosis (TUNEL positive cells) was decreased in relation to that delivered with sh-NC. Similar results were observed in the CIH-treated cells delivered with both miR-135a inhibitor and sh-MEG3 compared with that delivered with both miR-135a inhibitor and sh-NC. Therefore, we concluded that the silencing of MEG3 increased proliferation but inhibited apoptosis of endothelial cells of mice after CIH treatment by upregulating miR-135a.

Knock-down of MEG3 or HIF-1α alleviates aortic injury and cell apoptosis in CIH mice

RT-qPCR indicated that MEG3 was highly expressed in the aorta cells of CIH mice compared with normal mice, while the MEG3 expression was decreased in CIH mice injected with sh-MEG3 in contrast to CIH mice injected with sh-NC (*Figure 5A*). Western blot analysis revealed that the silencing of MEG3/HIF-1α or overexpression of miR-135a inhibited the expression of HIF-1α in CIH mice (*Figure 5B,C*). Moreover, compared with the CIH mice injected with sh-NC, the CIH mice injected with sh-MEG3 exhibited lower cleaved-caspase 3 and Bax expression and decreased TUNEL positive cell ratio, but higher PCNA and Bcl-2 expression in cells. The same trend was found in CIH mice injected with miR-135a agomir in contrast to CIH mice injected with agomir-NC (*Figure 5D,E,F,G*).

A

ENSGO00214548.8 (MEG3) (lncRNA, overlapping)

microRNA family	Seed position	Seed type	Transcript region	Repeat	Conservation		
					Primates	Mammals	Other vert
miR-135ab/135a-5p	chr14:101311805	7-mer-m8	ncRNA	no	78%	26%	0%
miR-135ab/135a-5p	chr14:101323680	8-mer	ncRNA	yes	56%	0%	0%

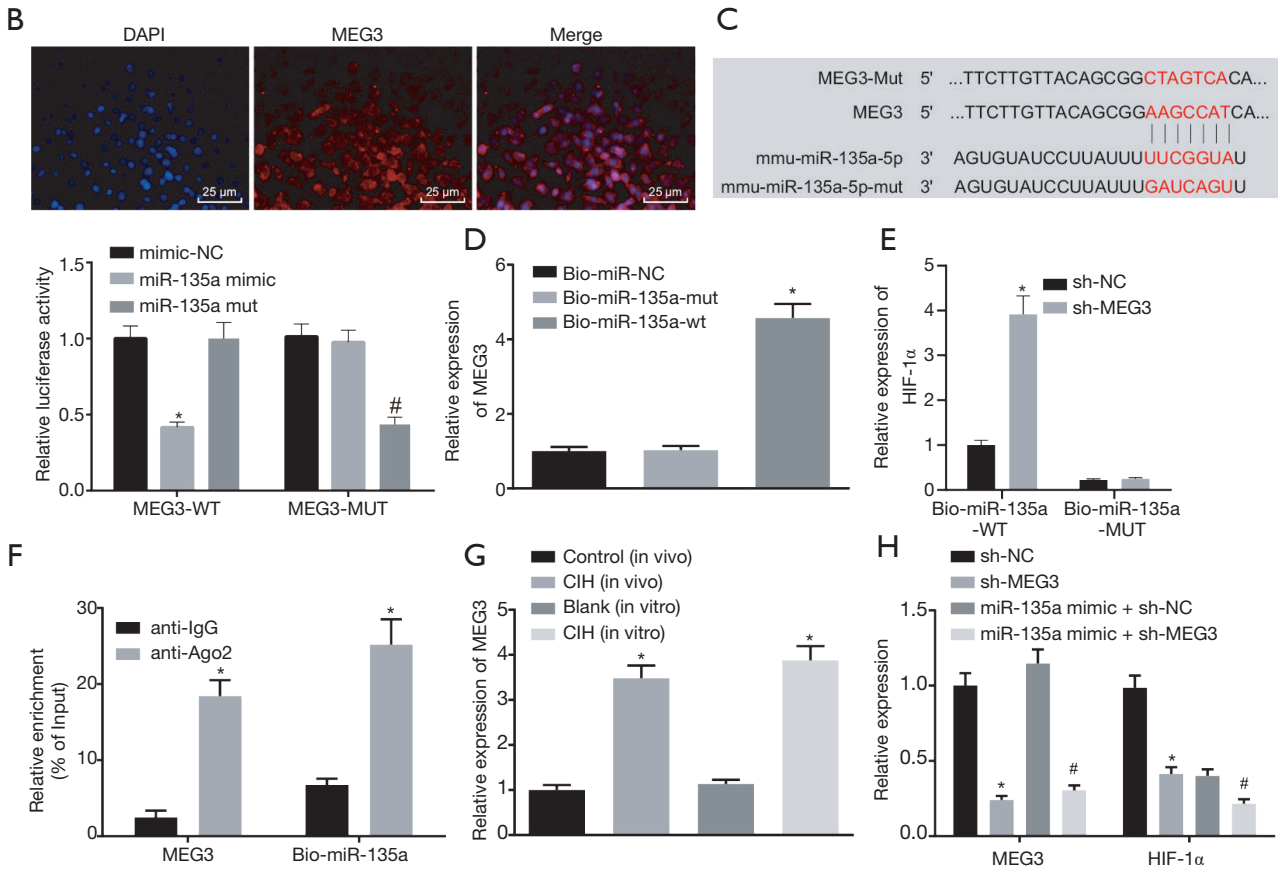

Figure 3 Silencing of MEG3 decreases HIF-1α expression by competitively binding to miR-135a in CIH. (A) The potential interaction between MEG3 and miR-135a predicted by an online website. (B) Subcellular localization of MEG3 by RNA-FISH. (C) The binding between MEG3 and miR-135a verified by dual-luciferase reporter gene assay. *, P<0.05 compared with the cells treated with mimic-NC; #, P<0.05 compared with the cells treated with miR-135a mimic. (D) The binding between MEG3 and miR-135a analyzed by RNA pull down. *, P<0.05 compared with the cells treated with NC-probe. (E) The role of MEG3 in the binding between miR-135a and HIF-1α analyzed by RNA pull down. *, P<0.05 compared with the cells treated with sh-NC. (F) The binding between MEG3 and miR-135a to Ago2 detected by RIP. *, P<0.05 compared with the cells treated with anti-IgG. (G) The MEG3 expression in mice and cells. *, P<0.05 compared with mice and cells without treatment. (H) The expression of MEG3 and HIF-1α in cells after different treatments examined by RT-qPCR. *, P<0.05 compared with cells treated with sh-NC; #, P<0.05 compared with cells treated with both miR-135a mimic and sh-NC. The results were measurement data and expressed as mean ± standard deviation. The data between two groups were analyzed by unpaired *t*-test and among multiple groups by ANOVA, with Tukey's *post hoc* test conducted. Each experiment was run in triplicate. CIH, chronic intermittent hypoxia; MEG3, maternally expressed gene 3; RIP, RNA immunoprecipitation; IgG, immunoglobulin G.

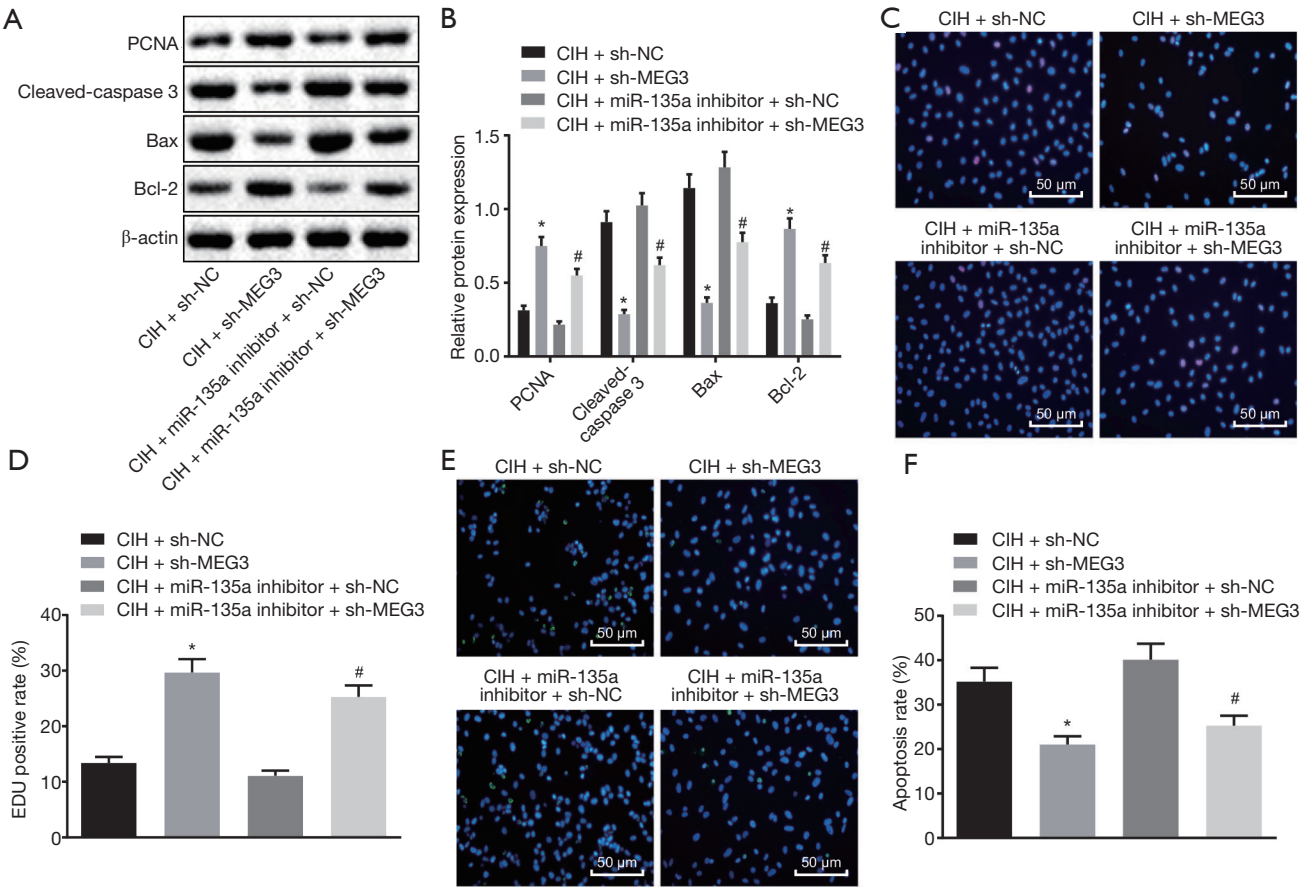

Figure 4 Silenced MEG3 promotes proliferation but inhibits apoptosis of endothelial cells of CIH mice via upregulation of miR-135a. (A,B) The protein expression of PCNA, Bcl-2, cleaved-caspase 3 and Bax in cells after different treatments. (C,D) Cell proliferation after different treatments examined by EdU assay (200×). (E,F) Cell apoptosis after different treatments examined by TUNEL staining (400×). *, P<0.05 compared with CIH-treated cells delivered with sh-NC; #, *, P<0.05 compared with CIH-treated cells delivered with both miR-135a inhibitor and sh-NC. The results were measurement data and expressed as mean ± standard deviation. The data between two groups were analyzed by unpaired *t*-test. Each experiment was run in triplicate. CIH, chronic intermittent hypoxia; MEG3, maternally expressed gene 3; Bcl-2, B-cell lymphoma 2; Bax, Bcl-2-associated X protein; EdU, 5-ethynyl-2'-deoxyuridine; TUNEL, terminal deoxynucleotidyl transferase-mediated dUTP nick end-labeling.

Furthermore, compared with the CIH mice injected with both miR-135a agomir and sh-NC, the CIH mice injected with both miR-135a agomir and sh-HIF-1α presented lower cleaved-caspase 3 and Bax expression and decreased TUNEL positive cell ratio, but higher PCNA and Bcl-2 expression in cells (*Figure 5D,E,F,G*). Moreover, HE staining showed that compared with the CIH mice treated with sh-NC, agomir-NC, or both miR-135a agomir and sh-NC, the CIH mice treated with sh-MEG3, miR-135a agomir, and both miR-135a agomir and sh-HIF-1α exhibited alleviated aortic injury, respectively (*Figure 5H*). Based on these findings, we concluded that the silencing of MEG3 or HIF-1α could suppress the aortic injury and cell apoptosis of CIH mice.

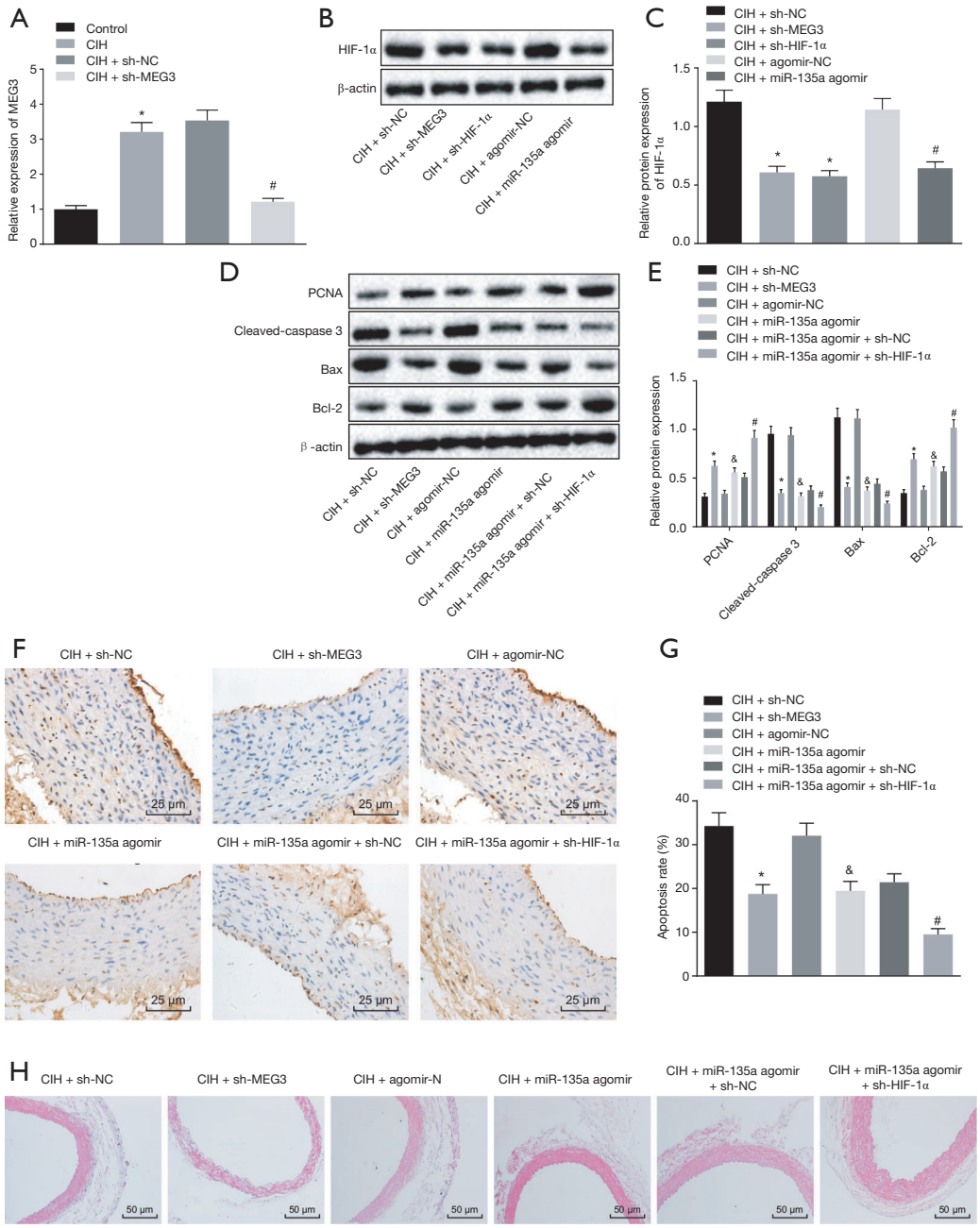

Figure 5 Silencing of MEG3/HIF-1α represses the aortic injury and cell apoptosis of CIH mice. (A) The MEG3 expression in CIH mice examined by RT-qPCR. *, P<0.05 compared with normal mice; #, P<0.05 compared with CIH mice treated with sh-NC. (B,C) The protein expression of HIF-1α in the aorta of mice after different treatments detected by western blot analysis. (D,E) the protein expression of PCNA, cleaved-caspase 3, Bax, and Bcl-2 in the aorta of mice after different treatments detected by western blot analysis. (F,G) Cell apoptosis in the aorta arch of mice after different treatments detected by TUNEL staining (400×). (H) The pathological changes of the aorta arch of mice after different treatments by HE staining (200×). (C,D,E,F,G): *, P<0.05 compared with CIH mice treated with sh-NC; #, P<0.05 compared with CIH mice treated with agomir-NC; &, P<0.05 compared with CIH mice treated with both miR-135a agomir and sh-NC. The results were measurement data and expressed as mean ± standard deviation. The data between two groups were analyzed by unpaired *t*-test and among multiple groups by ANOVA, with Tukey's *post hoc* test conducted. N=6. CIH, chronic intermittent hypoxia; MEG3, maternally expressed gene 3; Bcl-2, B-cell lymphoma 2; Bax, Bcl-2-associated X protein; TUNEL, terminal deoxynucleotidyl transferase-mediated dUTP nick end-labeling.

Discussion

CIH is defined as a unique pathological mechanism of OSA and is related to endothelial dysfunction and cardiovascular disorders (19,20). However, few studies have previously explored the involvement of lncRNAs and miRNAs in aortic endothelial dysfunction under CIH. Therefore, we conducted a tentative research through a series experiments and hypothesized that MEG3 affected aortic endothelial dysfunction in mice with CIH by mediating HIF-1α by interacting with miR-135a. Eventually, silencing of MEG3 inhibited endothelial injury and cell apoptosis in aorta of CIH mice by downregulating HIF-1α through sponging miR-135.

Initially, CIH induced endothelial dysfunction including aortic injury and cell apoptosis. Rats with CIH exhibited increased endothelial cell apoptosis in the aortic arches (2). CIH is also the main risk factor for endothelial dysfunction related to obstructive sleep apnea/hypopnea syndrome (OSAHS) (21). In this study, miR-135a was downregulated while HIF-1α was unregulated in CIH mice, and HIF-1α was the target gene of miR-135a. Similarly, the HIF-1α expression in the liver and eWAT was significantly upregulated in mice with CIH (22). Moreover, miR-135a has been found to target HIF-1α in bacterial meningitis, and to promote the proliferation and repress the apoptosis of astrocytes by targeting HIF-1α (7). The targeting relationship between HIF-1α and miR-135b has been shown to be essential in hypoxia-induced vascular endothelial injury (23).

In addition, MEG3 was found to competitively bind to miR-135a. The silencing of MEG3 could inhibit endothelial injury and cell apoptosis while promoting cell proliferation by downregulating HIF-1α. Moreover, miR-30a alleviated endothelial cell autophagy in CIH through translational regulation of Beclin-1, a primary inducer of endothelial dysfunction and injury (24). The effects of MEG3 on endothelial cells by interacting with miRNAs have been reported in numerous studies. For instance, MEG3 was reported to alleviate the senescence of vascular endothelial cells by impairing miR-128-mediated Girdin down-regulation (25). Furthermore, the inhibition of MEG3 enhanced cell proliferation and migration by upregulating miR-21 expression in a hypoxia cell model of PASMCs (11). Also, MEG3 has been shown to be involved in proliferation and apoptosis of neuroblastoma cells by regulating the pathway related to HIF-1α (26). Thus, these evidences with similar trend of our study could help prove the suppressive roles of MEG3 silencing in endothelial dysfunction by competitively binding to miR-135a via HIF-1α.

Moreover, upregulation of miR-135a or MEG3/HIF-1α silencing resulted in increased cell proliferation and decreased apoptosis as evidenced by high PCNA and Bcl-2 expression and low cleaved-caspase 3 and Bax expression in CIH-treated mice or cells. Bax and cleaved caspase-3 are regarded as pro-apoptotic factors while Bcl-2 has been identified as an anti-apoptosis factor (27). The increased expression of the Bcl-2/Bax ratio indicated reduced cell apoptosis, which was caused by H_2 in CIH-induced neurocognitive function injury (28). Furthermore, the silencing of MEG3 was revealed to increase the Bcl-2 levels but decrease the Bax levels in light-induced retinal degeneration (29). A former study showed that the silencing of miR-135a led to decreased Bcl-2 expression and increased Bax and caspase-3 expression in HUVECs, suggesting that overexpression of miR-135a could exert reverse effects (30).

Conclusions

Altogether, our findings show that the silencing of MEG3 suppressed apoptosis of aortic endothelial cells in mice with CIH via downregulation of HIF-1α by competitively binding to miR-135a (*Figure 6*). This study provides new insight into endothelial dysfunction under conditions of CIH. Nevertheless, it should be also pointed out that the efficacy and safety of MEG3 and miR-135 in clinical experiments are not clear yet, and that the specific mechanisms involving MEG3, miR-135a, and HIF-1α in the molecular and cellular network alterations in aortic endothelial injury in CIH still need to be elucidated by further studies. However, the evidence obtained in this study about the functional mechanisms of MEG3 and miR-135 provides new insights into the potential therapeutic approaches for the treatment of aortic endothelial injury in CIH.

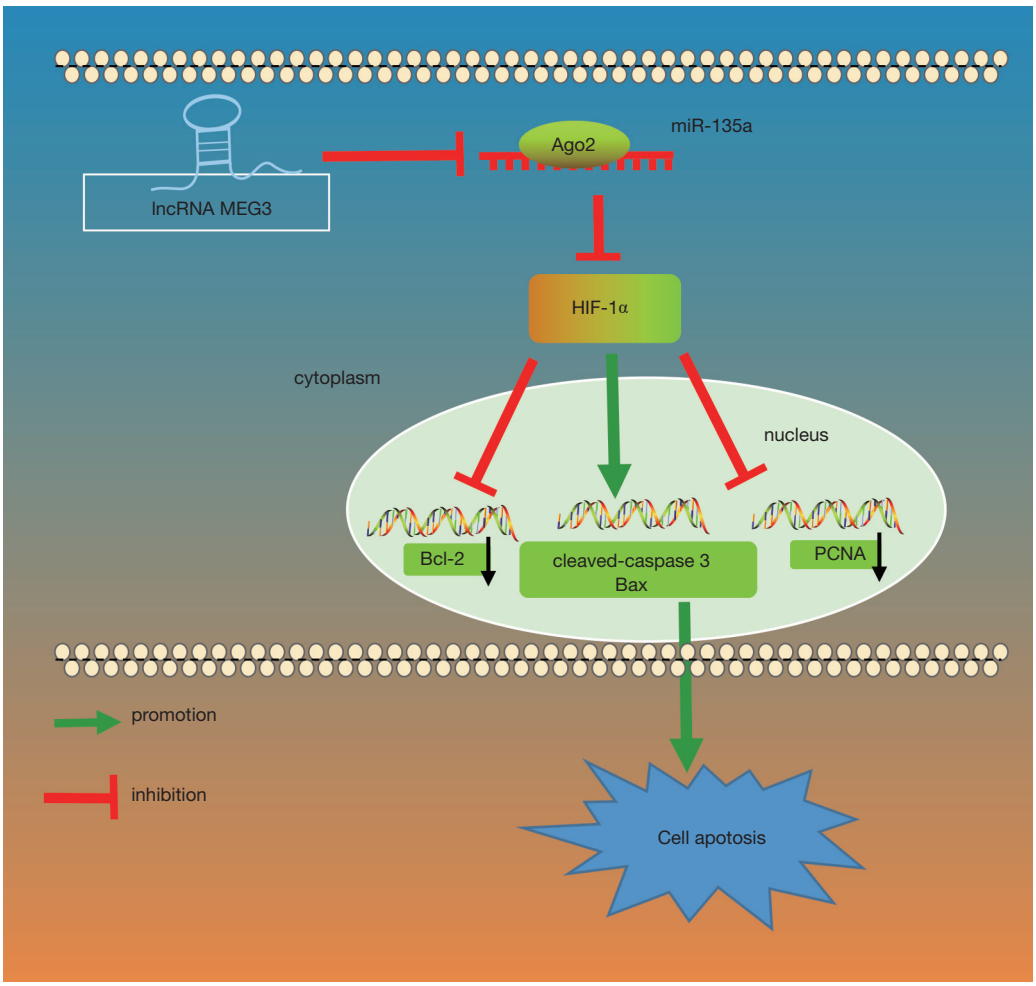

Figure 6 The molecular mechanism involving MEG3 in the regulation of CIH progression. MEG3 and HIF-1α were upregulated but miR-135a was downregulated in CIH. The silencing of MEG3 inhibited the HIF-1α expression by sponging miR-135 and decreased the protein expression of cleaved-caspase 3 and Bax but increased the protein expression of PCNA and Bcl-2, thus repressing the apoptosis of endothelial cells in the aorta tissues of CIH mice. CIH, chronic intermittent hypoxia; MEG3, maternally expressed gene 3; Bcl-2, B-cell lymphoma 2; Bax, Bcl-2-associated X protein; PCNA, proliferating cell nuclear antigen.

Acknowledgments

We would like to acknowledge the helpful comments on this paper received from our reviewers.

Funding: This work was supported by grant 2018-ZQN-55 for Medical Elite Cultivation Program of Fujian in China.

Footnote

Conflicts of Interest: All authors have completed the ICMJE uniform disclosure form (available at http://dx.doi.org/10.21037/jtd-19-2472). The authors have no conflicts of interest to declare.

Ethical Statement: The authors are accountable for all aspects of the work in ensuring that questions related to the accuracy or integrity of any part of the work are appropriately investigated and resolved. All animal experiments were performed following the principles and procedures of the Guide for the Care and Use of Laboratory Animals by the National Institutes of Health. This study was approved by the Animal Ethics Committee of The First Affiliated Hospital of Fujian Medical University (No.

201806003).

References

1. Navarrete-Opazo A, Mitchell GS. Therapeutic potential of intermittent hypoxia: a matter of dose. Am J Physiol Regul Integr Comp Physiol 2014;307:R1181-97.
2. Ren J, Liu W, Deng Y, et al. Losartan attenuates aortic endothelial apoptosis induced by chronic intermittent hypoxia partly via the phospholipase C pathway. Sleep Breath 2017;21:679-89.
3. Zhou S, Wang Y, Tan Y, et al. Deletion of metallothionein exacerbates intermittent hypoxia-induced oxidative and inflammatory injury in aorta. Oxid Med Cell Longev 2014;2014:141053.
4. Polotsky VY, Savransky V, Bevans-Fonti S, et al. Intermittent and sustained hypoxia induce a similar gene expression profile in human aortic endothelial cells. Physiol Genomics 2010;41:306-14.
5. Yang YY, Shang J, Liu HG. Role of endoplasmic reticular stress in aortic endothelial apoptosis induced by intermittent/persistent hypoxia. Chin Med J (Engl) 2013;126:4517-23.
6. Martinez CA, Kerr B, Jin C, et al. Obstructive Sleep Apnea Activates HIF-1 in a Hypoxia Dose-Dependent Manner in HCT116 Colorectal Carcinoma Cells. Int J Mol Sci 2019. doi: 10.3390/ijms20020445.
7. Dong Y, Wang J, Du KX, et al. MicroRNA-135a participates in the development of astrocytes derived from bacterial meningitis by downregulating HIF-1α. Am J Physiol Cell Physiol 2019;316:C711-C721.
8. Liu KX, Chen GP, Lin PL, et al. WITHDRAWN: Detection and analysis of apoptosis- and autophagy-related miRNAs of vascular endothelial cells in a mouse chronic intermittent hypoxia model. Life Sci 2016. doi: 10.1016/j.lfs.2016.08.005.
9. Icli B, Wu W, Ozdemir D, et al. MicroRNA-135a-3p regulates angiogenesis and tissue repair by targeting p38 signaling in endothelial cells. FASEB J 2019;33:5599-614.
10. Boulberdaa M, Scott E, Ballantyne M, et al. A Role for the Long Noncoding RNA SENCR in Commitment and Function of Endothelial Cells. Mol Ther 2016;24:978-90.
11. Zhu B, Gong Y, Yan G, et al. Down-regulation of lncRNA MEG3 promotes hypoxia-induced human pulmonary artery smooth muscle cell proliferation and migration via repressing PTEN by sponging miR-21. Biochem Biophys Res Commun 2018;495:2125-32.
12. Tan J, Xiang L, Xu G. LncRNA MEG3 suppresses migration and promotes apoptosis by sponging miR-548d-3p to modulate JAK-STAT pathway in oral squamous cell carcinoma. IUBMB Life 2019;71:882-90.
13. Wu Z, He Y, Li D, et al. Long noncoding RNA MEG3 suppressed endothelial cell proliferation and migration through regulating miR-21. Am J Transl Res 2017;9:3326-35.
14. Jun J, Reinke C, Bedja D, et al. Effect of intermittent hypoxia on atherosclerosis in apolipoprotein E-deficient mice. Atherosclerosis 2010;209:381-6.
15. Drager LF, Li J, Shin MK, et al. Intermittent hypoxia inhibits clearance of triglyceride-rich lipoproteins and inactivates adipose lipoprotein lipase in a mouse model of sleep apnoea. Eur Heart J 2012;33:783-90.
16. Reinke C, Bevans-Fonti S, Drager LF, et al. Effects of different acute hypoxic regimens on tissue oxygen profiles and metabolic outcomes. J Appl Physiol (1985) 2011;111:881-90.
17. Livak KJ, Schmittgen TD. Analysis of relative gene expression data using real-time quantitative PCR and the 2(-Delta Delta C(T)) Method. Methods 2001;25:402-8.
18. Wang K, Long B, Zhou LY, et al. CARL lncRNA inhibits anoxia-induced mitochondrial fission and apoptosis in cardiomyocytes by impairing miR-539-dependent PHB2 downregulation. Nat Commun 2014;5:3596.
19. Yang X, Zhang L, Liu H, et al. Cardiac Sympathetic Denervation Suppresses Atrial Fibrillation and Blood Pressure in a Chronic Intermittent Hypoxia Rat Model of Obstructive Sleep Apnea. J Am Heart Assoc 2019;8:e010254.
20. Badran M, Golbidi S, Devlin A, et al. Chronic intermittent hypoxia causes endothelial dysfunction in a mouse model of diet-induced obesity. Sleep Med 2014;15:596-602.
21. Liu KX, Chen GP, Lin PL, et al. Detection and analysis of apoptosis- and autophagy-related miRNAs of mouse vascular endothelial cells in chronic intermittent hypoxia model. Life Sci 2018;193:194-9.
22. Thomas A, Belaidi E, Moulin S, et al. Chronic Intermittent

Hypoxia Impairs Insulin Sensitivity but Improves Whole-Body Glucose Tolerance by Activating Skeletal Muscle AMPK. Diabetes 2017;66:2942-51.
23. Yang S, Yin J, Hou X. Inhibition of miR-135b by SP-1 promotes hypoxia-induced vascular endothelial cell injury via HIF-1alpha. Exp Cell Res 2018;370:31-8.
24. Bi R, Dai Y, Ma Z, et al. Endothelial cell autophagy in chronic intermittent hypoxia is impaired by miRNA-30a-mediated translational control of Beclin-1. J Cell Biochem 2019;120:4214-24.
25. Lan Y, Li YJ, Li DJ, et al. Long noncoding RNA MEG3 prevents vascular endothelial cell senescence by impairing miR-128-dependent Girdin downregulation. Am J Physiol Cell Physiol 2019;316:C830-C843.
26. Tang W, Dong K, Li K, et al. MEG3, HCN3 and linc01105 influence the proliferation and apoptosis of neuroblastoma cells via the HIF-1alpha and p53 pathways. Sci Rep 2016;6:36268.
27. Mo WL, Chai CZ, Kou JP, et al. Sheng-Mai-San attenuates contractile dysfunction and structural damage induced by chronic intermittent hypoxia in mice. Chin J Nat Med 2015;13:743-50.
28. Li W, Yang S, Yu FY, et al. Hydrogen ameliorates chronic intermittent hypoxia-induced neurocognitive impairment via inhibiting oxidative stress. Brain Res Bull 2018;143:225-33.
29. Zhu YX, Yao J, Liu C, et al. Long non-coding RNA MEG3 silencing protects against light-induced retinal degeneration. Biochem Biophys Res Commun 2018;496:1236-42.
30. Yan X, Li W, Yang L, et al. MiR-135a Protects Vascular Endothelial Cells Against Ventilator-Induced Lung Injury by Inhibiting PHLPP2 to Activate PI3K/Akt Pathway. Cell Physiol Biochem 2018;48:1245-58.

Cite this article as: Ding H, Huang J, Wu D, Zhao J, Huang J, Lin Q. Silencing of the long non-coding RNA MEG3 suppresses the apoptosis of aortic endothelial cells in mice with chronic intermittent hypoxia via downregulation of HIF-1α by competitively binding to microRNA-135a. J Thorac Dis 2020;12(5):1903-1916. doi: 10.21037/jtd-19-2472